

Similarity-Based Random Partition Distribution for Clustering Functional Data

Tomoya Wakayama*¹, Shonosuke Sugasawa², and Genya Kobayashi³

¹Graduate School of Economics, The University of Tokyo

²Faculty of Economics, Keio University

³School of Commerce, Meiji University

Abstract

Random partition distribution is a crucial tool for model-based clustering. This study advances the field of random partition in the context of functional spatial data, focusing on the challenges posed by hourly population data across various regions and dates. We propose an extended generalized Dirichlet process, named the similarity-based generalized Dirichlet process (SGDP), to address the limitations of simple random partition distributions (e.g., those induced by the Dirichlet process), such as an overabundance of clusters. This model prevents excess cluster production as well as incorporates pairwise similarity information to ensure accurate and meaningful grouping. The theoretical properties of the SGDP are studied. Then, SGDP-based random partition is applied to a real-world dataset of hourly population flow in 500m² meshes in the central part of Tokyo. In this empirical context, our method excels at detecting meaningful patterns in the data while accounting for spatial nuances. The results underscore the adaptability and utility of the method, showcasing its prowess in revealing intricate spatiotemporal dynamics. The proposed SGDP will significantly contribute to urban planning, transportation, and policy-making and will be a helpful tool for understanding population dynamics and their implications.

Keywords: functional data analysis, generalized Dirichlet process, pairwise similarity, population data, spatiotemporal data

*Corresponding Author: tom-w9@g.ecc.u-tokyo.ac.jp

1 Introduction

The past few decades have witnessed a rapid proliferation of mobile devices. The resulting surge in fine population data is pivotal for comprehending and planning the foundational aspects of contemporary society. Specifically, it encompasses various domains, including urban and transportation planning, healthcare service distribution, and extensive policy-making (Páez and Scott, 2004; Wang and Mu, 2018; Ahmadi-Javid et al., 2018). The collection and analysis of population data also hold economic significance. By meticulously analyzing population data, understanding consumer behavioral patterns and preferences becomes feasible, which aids in developing and executing marketing strategies (Pol, 1986; Nagata et al., 2013). Thus, effectively utilizing population statistics is imperative for societal advancement.

Clustering is a viable technique to distill meaningful insights from population data. Identifying groups and commonalities within groups and unveiling regional traits can contribute to both industry, such as ridesharing services and street advertising, and research, including urban engineering and humanities. In particular, model-based clustering is compatible with nonparametric Bayesian methods. Dirichlet process (DP)-based clustering, as introduced by Ferguson (1973, 1974), can autonomously ascertain cluster quantities and incorporate spatial structures. The seminal study of Dahl et al. (2017) adeptly integrated geographical proximity when assigning existing clusters to new items within the Pitman–Yor process (Ishwaran and James, 2001; Pitman and Yor, 1997), contributing to valuable applications (Glynn et al., 2021; Grazian, 2023). Notably, adjacency information is crucial in population data analysis (Lym, 2021; Zhang et al., 2019), and a high correlation is observed between neighboring districts, as depicted in Figure 1.

Nonetheless, two primary attributes of our dataset, i.e., its multivariate nature and the presence of temporal information, impede the application of existing methods to it. When tackling multivariate clustering problems, naively applying methods that do not fix the number of clusters leads to the creation of excess clusters and is inappropriate. Owing to their inherent complexity, high-dimensional data are readily classifiable, a trait that aids in supervised classification tasks (Delaigle and Hall, 2012; Wakayama and Imaizumi, 2024). Conversely, this high classifiability may lead to an excessive number of groups in unsupervised

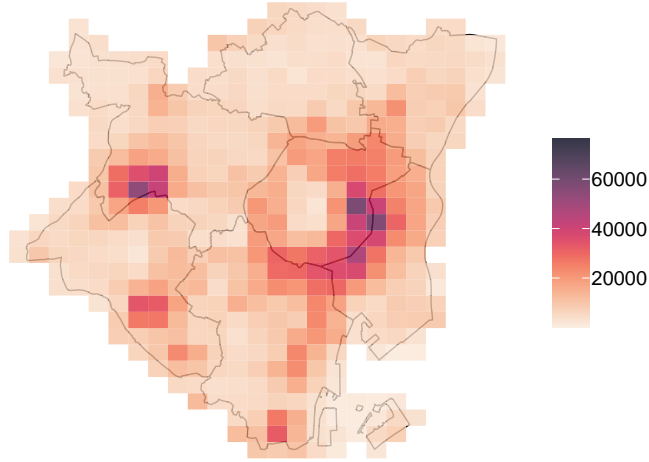


Figure 1: Population in the central districts of Tokyo at 2 PM on January 29, 2019 (Japan Standard Time, JST).

clustering. In particular, this property would accelerate the tendency of the DP to favor smaller cluster sizes and create superfluous clusters (Miller and Harrison, 2013, 2014), thereby hindering the extraction of beneficial knowledge from the data. Shifting the focus to the temporal aspect reveals that considering the spatial structures alone is inadequate. Figure 2 depicts the hourly population flow of a week in a specific area. The intra-day pattern may vary between weekdays and holidays or owing to pre-holiday effects such as the “Happy Friday” phenomenon (Stutz, 2004; Lu and Reddy, 2012). In such scenarios, group structures vary over time, and vital insights could be missed by focusing only on typical weekday trends.

To address these challenges, we propose a similarity-based random partition distribution using a generalized Dirichlet process (GDP, Hjort, 2000), namely similarity-based GDP (SGDP), and cluster the observed hourly population flow as functional data, which are realizations of stochastic processes. Our methodology reduces the risk of over-clustering through generalized parameterization (Rodriguez and Dunson, 2014), and it integrates geographic adjacency, which is explored theoretically in this study. Furthermore, we model the discrepancy between observations and the group mean using a Gaussian process. Intuitively, if a value deviates from the group mean at a particular time in a region, then the effect naturally spreads to the contiguous times as well. Technically, if the gap is assumed to be independent noise, then the similarity (likelihood) between the observation and the group mean will be overly small, resulting from the calculated product of the likelihoods for the number of observations. However, this issue is less pronounced in Gaussian processes, as they account for correlations. Additionally, our model adapts to temporal variations, enabling

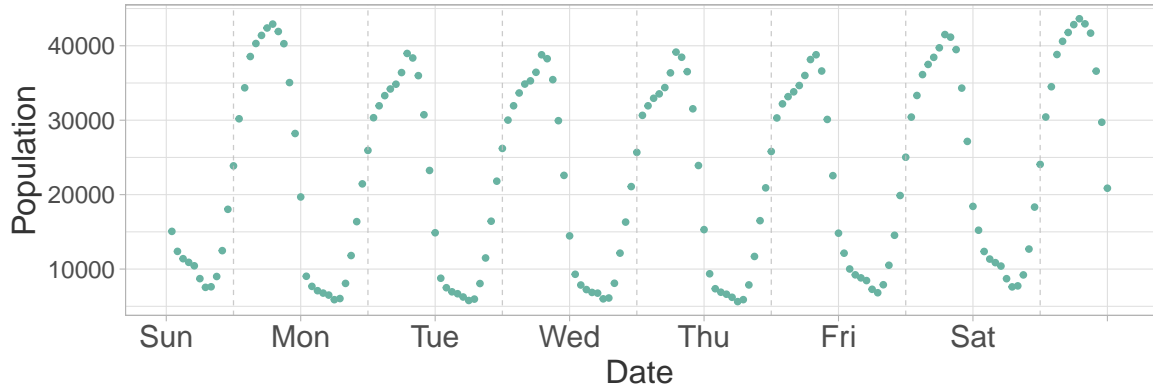


Figure 2: Hourly population flow in a week in a certain mesh.

the identification of time-series cluster shifts. This approach facilitates a nuanced capture of the distinctive characteristics of each region.

The remainder of this paper is structured as follows. Section 2 reviews the GDP, delineates a similarity-based random partition and discusses its properties. In Section 3, we introduce the proposed model for clustering spatial functional data, detailing the prior distribution setup and the computation of the posterior distribution. Sections 4 and 5 describe the simulation experiments and apply the model to population data, presenting the empirical findings. Section 6 discusses the major conclusions drawn from the study findings and presents future research directions. The Julia code used to implement the proposed methods is publicly available in the GitHub repository (<https://github.com/TomWaka/Similarity-based-Generalized-Dirichlet-Process>).

2 Similarity-based random partition distribution

2.1 GDP and induced partition distribution

To construct the GDP, we employ a stick-breaking construction, reflective of its discrete nature (Hjort, 2000; Rodriguez and Dunson, 2014). A probability measure G is defined as a GDP if it follows the following formulation:

$$G(\cdot) = \sum_{h=1}^{\infty} w_h \delta_{m_h}(\cdot),$$

where $w_h = v_h \prod_{\ell=1}^{h-1} (1 - v_\ell)$, $v_h \sim Be(\alpha\beta, \alpha(1 - \beta))$, $m_h \sim G_0$, $\alpha \in \mathbb{R}_+$, and $\beta \in (0, 1)$. G_0 refers to a nonatomic probability measure, often termed a base measure of G , and all $\{v_h\}_{h \geq 1}, \{m_h\}_{h \geq 1}$ are independent. In this configuration, we denote the probability distribution as $GDP(\alpha\beta, \alpha(1 - \beta), G_0)$. In the scenario where $\alpha\beta = 1$, G is reduced to the DP (Ferguson, 1973, 1974; Sethuraman, 1994; Ishwaran and James, 2001; Müller et al., 2015).

Suppose we have n items $\{1, 2, \dots, n\}$ independently sampled from $GDP(\alpha\beta, \alpha(1 - \beta), G_0)$ and partitioned into k distinct groups (N_1, \dots, N_k) , where N_j represents the cardinality of the j th group for $j = 1, \dots, k$. As the GDP is a partially exchangeable distribution, the predictive probability function of assignment z_{n+1} can be explicitly obtained as follows (Pitman, 1995; Barcella et al., 2017):

$$\begin{aligned} p(z_{n+1} = j \mid z_1, \dots, z_n) &= \frac{\alpha\beta + N_j - 1}{\alpha + n - 1} \prod_{\ell=1}^{j-1} \frac{\alpha(1 - \beta) + \sum_{m=\ell+1}^k N_m}{\alpha + \sum_{m=\ell+1}^k N_m - 1} \quad \text{for } 1 \leq j \leq k, \\ p(z_{n+1} = k + 1 \mid z_1, \dots, z_n) &= \frac{\alpha(1 - \beta)}{\alpha + n - 1} \prod_{\ell=1}^{k-1} \frac{\alpha(1 - \beta) + \sum_{m=\ell+1}^k N_m}{\alpha + \sum_{m=\ell+1}^k N_m - 1}, \end{aligned} \quad (1)$$

where z_1, \dots, z_n are the grouping assignments, $N_j = \sum_{i=1}^n I(z_i = j)$, and $I(\dots)$ is an indicator function. The expression (1) comprises two scenarios: the first detailing the probability of a new item being stored as an existing cluster, and the second regarding the probability of it being assigned to a new group. Expression (1) demonstrates that the joint probability of (z_1, \dots, z_n) can be depicted as

$$p(z_1, \dots, z_n; \alpha, \beta) = \prod_{i=1}^n p(z_i \mid z_1, \dots, z_{i-1}; \alpha, \beta),$$

where

$$\begin{aligned} p(z_i = j \mid z_1, \dots, z_{i-1}; \alpha, \beta) &= \frac{\alpha\beta + N_j(i) - 1}{\alpha + i - 2} \prod_{\ell=1}^{j-1} A_\ell(i), \quad j = 1, \dots, k, \\ p(z_i = k + 1 \mid z_1, \dots, z_{i-1}; \alpha, \beta) &= \frac{\alpha(1 - \beta)}{\alpha + i - 2} \prod_{\ell=1}^{k-1} A_\ell(i), \end{aligned} \quad (2)$$

and

$$A_\ell(i) = \frac{\alpha - \alpha\beta + \sum_{m=\ell+1}^k N_m(i)}{\alpha - 1 + \sum_{m=\ell+1}^k N_m(i)}, \quad \ell = 1, \dots, j - 1,$$

where $k = k(i)$ denotes the number of clusters induced by z_1, \dots, z_{i-1} , and $N_m(i)$ indicates the size of the m th cluster induced by z_1, \dots, z_{i-1} . When $\alpha\beta = 1$, $A_\ell(i) = 1$ for all ℓ and i , suggesting that the distribution (2) is equal to the Ewens distribution (Ewens, 1972; Pitman, 1995, 1996).

The number of partitions constructed by the GDP depends on n , α , and β . Rodriguez and Dunson (2014) proved that when $\alpha\beta > 1$, the expected number of partitions remains finite even if n diverges. Intuitively, because the lower case of (1) is a decreasing function of $\alpha\beta$, if $\alpha\beta$ is large, a new group is unlikely to be generated, indicating a significant departure from the scenario $\alpha\beta = 1$, that is, the standard DP, where $k \approx \log n$ as n approaches infinity (Korwar and Hollander, 1973; Antoniak, 1974). Such flexibility in controlling the growth in the number of clusters is crucial for limiting an excessive number of clusters during clustering.

2.2 Introducing pairwise similarity in random partition

Next, we extend the GDP-based random partition to incorporate pairwise information. Here, we consider the scenario where pairwise similarity information $s_{ii'}(\tau)$, such as covariate distance or contingency information, exists for each pair of items $i, i' = 1, \dots, n$. In the application described in Section 5, we define $s_{ii'} = 1$ for adjacent areas and $s_{ii'} = \tau \in (0, 1)$ otherwise. The objective is to embed s_{ij} into the prior distribution of z_1, \dots, z_n such that two subjects with large values of $s_{ii'}$ are more likely to belong to the same cluster. We then extend the conditional probability given in (2) as the following SGDP-based random partition distribution:

$$p_\omega(z_i = j \mid z_1, \dots, z_{i-1}; \alpha, \beta) = \omega_j(i) \cdot \frac{\alpha\beta + N_j(i) - 1}{\alpha + i - 2} \prod_{\ell=1}^{j-1} A_\ell(i), \quad (3)$$

for the i th item as an existing cluster $j \in \{1, \dots, k\}$, where

$$\omega_j(i) = \left(\frac{\sum_{j'=1}^k (\alpha\beta + N_{j'}(i) - 1) \prod_{\ell=1}^{j'-1} A_\ell(i)}{\sum_{j'=1}^k \omega_{j'}^*(i) (\alpha\beta + N_{j'}(i) - 1) \prod_{\ell=1}^{j'-1} A_\ell(i)} \right) \omega_j^*(i), \quad j = 1, \dots, k \quad (4)$$

and

$$\omega_j^*(i) = \frac{\sum_{i'=1}^{i-1} I(z_{i'} = j) \lambda(s_{ii'})}{\sum_{i'=1}^{i-1} \lambda(s_{ii'})}, \quad (5)$$

where $\lambda(\cdot) : \mathbb{R} \rightarrow \mathbb{R}$ denotes an increasing function. Although λ can be any increasing function, we adopt the identity function in our experiments in Sections 4 and 5. Importantly, the transformation (4) of the original similarity weight $\omega_j^*(i)$ to $w_j(i)$ lets (3) act as a proper probability distribution and does not impact the relative magnitude because $w_j(i) \propto \omega_j^*(i)$.

Additionally, for this formulation, the following expression holds:

$$\sum_{j=1}^k p_\omega(z_i = j \mid z_1, \dots, z_{i-1}; \alpha, \beta) = \sum_{j=1}^k \frac{\alpha\beta + N_j(i) - 1}{\alpha + i - 2} \prod_{\ell=1}^{j-1} A_\ell(i),$$

for $i = 1, \dots, n$, aligning with the probability of assigning z_i to existing clusters under the standard GDP (absence of the similarity measure). Hence, the conditional probability of assigning z_n to a new cluster is expressed in (2), which remains unaffected by the similarity weight $\omega_j^*(i)$. Consequently, the similarity measure does not affect the growth in the number of clusters, and the role of the similarity measure is independent of those of α and β ; this feature is preferable in terms of the interpretability of the parameters (Dahl et al., 2017).

2.3 Properties of SGDP

Here, we discuss the properties of the SGDP-based random partition distribution defined in (3). First, we focus on the probability of creating a new cluster. For a given cluster, the probability of a new cluster occurring for GDP- and SGDP-based partition is identical:

$$p_\omega(z_{i+1} = k + 1 \mid z_1, \dots, z_i) = \frac{\alpha - \alpha\beta}{\alpha + i - 1} \prod_{\ell=1}^{k-1} \frac{\alpha - \alpha\beta + \sum_{m=\ell+1}^k N_m}{\alpha - 1 + \sum_{m=\ell+1}^k N_m},$$

irrespective of λ and τ . If $\beta \in (0, 1)$ is large, then the first term becomes small. Additionally, when $\alpha\beta > 1$, each term of the $k - 1$ products is less than 1, indicating that α and β are pivotal in controlling the cluster quantity during SGDP-based partitioning.

Subsequently, we assess the impact of the similarity measure (adjacency structure). According to the formulation of (3), similarity does not affect the probability of new cluster creation for each allocation. We designed (3) to emphasize spatial proximity when assigning the group to which a new item should be assigned among existing groups. This feature is corroborated by the following two results.

Proposition 1. *For fixed parameters $\alpha > 0, \beta \in (0, 1), \tau > 0$, and any partition, a new item*

i has an increased prior probability of entering a cluster with more adjacent items.

Proof. To simplify the notation, Equation (3) is expressed as follows:

$$p_{\omega}(z_i = j \mid z_1, \dots, z_{i-1}; \alpha, \beta) = C_{1,ij} \omega_j(i).$$

In particular, $C_{1,ij}$ does not include similarity information. Thereafter, we obtain

$$\begin{aligned} \omega_j(i) &= \left(\frac{\sum_{j'=1}^k (\alpha\beta + i - 2) \prod_{\ell=1}^{j'-1} A_{\ell}(i)}{\sum_{j'=1}^k \omega_j^*(i) (\alpha\beta + i - 2) \prod_{\ell=1}^{j'-1} A_{\ell}(i)} \right) \omega_j^*(i) \\ &= C_{2,ij} \omega_j^*(i), \end{aligned}$$

where $C_{2,ij}$ is independent of similarity information as well. Hence, the role of similarity information in allocation is solely through $\omega_j^*(i)$, attributed to the following definition:

$$\omega_j^*(i) = \frac{\sum_{i'=1}^{i-1} I(z_{i'} = j) \lambda(s_{ii'})}{\sum_{i'=1}^{i-1} I(z_{i'} = j) \lambda(s_{ii'}) + \sum_{i'=1}^{i-1} I(z_{i'} \neq j) \lambda(s_{ii'})}.$$

$p_{\omega}(z_i = j \mid z_1, \dots, z_{i-1}; \alpha, \beta)$ increases with the number of items adjacent to item i within cluster j . □

Proposition 2. *For random sets α, β, τ and partitions, a new element i has an increased marginal probability of being assigned to a cluster with more neighboring districts.*

Proof. The marginal distribution is computed as the integral of the product of the probability that item i belongs to cluster j given the parameters and the probability distribution of these parameters. To prove this relationship, confirming that the derivative of the marginal distribution of $\omega_j^*(i)$ is positive is sufficient, which is verified by the Leibniz integral rule (Folland, 1999) and the results of Proposition 1. □

These findings confirm that the prior distribution appropriately incorporates spatial information. Additionally, in the posterior distribution, in the process of aligning data and clusters, inherently close districts can be placed in the same group; however, the observed data may deviate slightly (owing to noise).

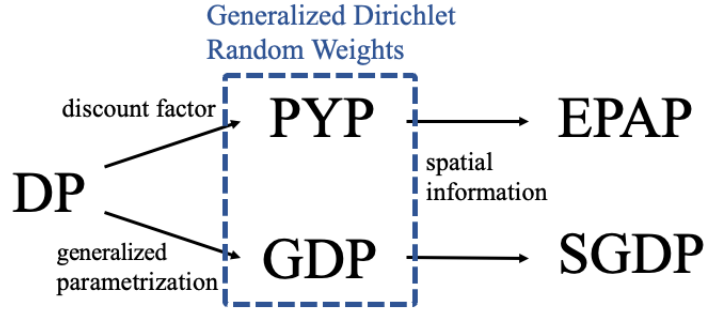


Figure 3: Diagram of random partition distributions. The relationships between Dirichlet process (DP), Pitman–Yor process (PYP), generalized Dirichlet process (GDP), Ewens–Pitman attraction process (EPAP), and similarity-based GDP (SGDP).

2.4 Comparison with other distributions

We explore the relationship between our partition distribution and existing frameworks, as depicted in Figure 3. Setting $\alpha\beta = 1$ in the proposed distribution yields alignment with the Ewens–Pitman attraction distribution with a discount of 0, developed by Dahl et al. (2017). A fundamental divergence from this approach is our adoption of the GDP rather than the Pitman–Yor process. While GDP and the Pitman–Yor process fall under the same category of Generalized Dirichlet Random Weights (Connor and Mosimann, 1969; Ishwaran and James, 2001), they are differentiated by their parametrization philosophies. The GDP signifies a straightforward relaxation of the model constraints, whereas the Pitman–Yor process revises the DP’s “rich-get-richer” paradigm through the incorporation of a discount factor. The choice of model philosophy is predominantly determined by the specific attributes of the dataset and analytical objectives.

Considering the attributes of alternative distributions and datasets is instructive to comprehend the rationale for employing GDP-based methodologies. Primarily, in the DP, the number of clusters increases at a logarithmic rate of the sample size (Korwar and Hollander, 1973; Antoniak, 1974). Both practical and theoretical evidences suggest that the DP’s tendency to finely differentiate data often results in an excessive number of clusters (Miller and Harrison, 2013). Moreover, the Pitman–Yor process, characterized by its power-law tail decay, encounters similar challenges (Pitman and Yor, 1997; Ayed et al., 2019; Miller and Harrison, 2014). Subsequently, the dataset of primary interest in this context is functional data, notably high-dimensional. Owing to their intricate structures, functional data are readily classifiable, thus benefitting supervised classification tasks (Delaigle and Hall, 2012;

Wakayama and Imaizumi, 2024). However, in clustering scenarios where the number of clusters is indeterminate, such high dimensionality may engender an overabundance of clusters. Consequently, the intrinsic nature of the DP could be exacerbated by the functional data, and thus, using a GDP-based method is preferable (Rodriguez and Dunson, 2014). We refrain from setting $\alpha\beta$ to 1 or lower. Instead, we advocate for either constructing the prior distribution so that $\alpha\beta$ exceeds 1 or fixing it at a value greater than 1.

3 Clustering functional data with the SGDP

3.1 Model settings

Let $y_1(x), \dots, y_n(x)$ represent functional observations for $x \in \mathcal{X}$. We consider the following model-based clustering:

$$\begin{aligned}
 y_i(x) \mid \mu_i(x) &\sim \mathcal{GP}(\mu_i(x), C_y), \quad \mu_i(x) = \sum_{j=1}^{K_n} \theta_j(x) I(z_i = j), \quad i = 1, \dots, n \\
 \theta_j(x) &\sim \mathcal{GP}(m_\theta, C_\theta), \quad j = 1, \dots, K_n, \quad (z_1, \dots, z_n) \sim \text{SGDP}(\alpha, \beta, \tau),
 \end{aligned} \tag{6}$$

where \mathcal{GP} denotes Gaussian process, $\mu_i(\cdot)$ is the mean function of $y_i(x)$, $C_y(\cdot)$ is the covariance function of the error term, K_n is the number of clusters, z_1, \dots, z_n are membership variables, $\theta_j(\cdot)$ is the common mean function within the j th cluster, $m_\theta(\cdot)$ is the overall mean function, and $C_\theta(\cdot)$ is the covariance function. Here, $\text{SGDP}(\alpha, \beta, \tau)$ denotes the SGDP with parameters α , β , and τ , that is, the membership variables follow a prior random partition distribution (3). A gamma prior distribution is placed on α , and beta prior distributions are placed on β and τ . Regarding m_θ , we impose a $\mathcal{GP}(m_m, C_m)$ prior. If we assume a Radial Basis Function (RBF) (e.g., Rasmussen and Williams, 2006), $K(x, x') = \eta^2 \exp(-\|x - x'\|^2 / \phi^2)$, for covariance matrices C_y and C_θ , then the scale parameters η_y and η_θ have conjugate priors: inverse-gamma distributions. As for the range parameters ϕ_y and ϕ_θ , arbitrary prior distributions reflecting analysts' beliefs can be used. If the data are observed repeatedly T times in each area i (e.g., if the functions are observed daily), y_i can be replaced with y_{it} and μ_i with μ_{it} ($t = 1, \dots, T$).

3.2 Posterior computation

We present an algorithm for simulating the posterior distribution of the nonparametric Bayesian model in (6). While this model offers a powerful framework for nonlinear regression and clustering, posterior inference is complicated by the infinite-dimensional nature of the Gaussian process and lack of a straightforward stick-breaking representation. To circumvent these challenges, namely the Gaussian process, we consider a finite-dimensional approximation to the Gaussian process based on a finite set of measurement points $\mathbf{x} \subset \mathcal{X}$. Then, the joint posterior distribution is represented as follows:

$$\prod_{i=1}^n p(y_i(\mathbf{x}) \mid \mu_i(\mathbf{x}), C_y) \times \pi(z_1, \dots, z_n, K_n = k \mid \alpha, \beta, \tau) \\ \times \prod_{j=1}^{K_n} \pi(\theta_j(\mathbf{x}) \mid m(\mathbf{x}), C_\theta(\mathbf{x})) \times \pi(\alpha, \beta, \tau, \eta_\theta, \phi_\theta, \eta_y, \phi_y).$$

While some nonparametric Bayesian models admit efficient posterior simulation via specialized algorithms (MacEachern and Müller, 1998; Ishwaran and Zarepour, 2000; Neal, 2000; Müller et al., 2015), the non-exchangeability and complex form of our formulation preclude such approaches. Therefore, we resort to a general-purpose Markov chain Monte Carlo (MCMC) technique, the Gibbs sampler (Gelfand and Smith, 1990), which iteratively samples each parameter from its full conditional distribution given the current values of all the other parameters.

Most parameters can be updated by exploiting conjugacy. In particular, the cluster-specific GP atoms θ_j can be sampled from multivariate Gaussian full conditionals:

$$p(\theta_j \mid \cdot) \propto \pi(\theta_j(\mathbf{x}) \mid m(\mathbf{x}), C_\theta(\mathbf{x})) \prod_{i:z_i=j} p(y_i \mid \theta_j(\mathbf{x}), C_y(\mathbf{x})) \\ \propto N(m_{pos}, C_{pos}),$$

where $C_{pos} = \{C_\theta^{-1} + N_j C_y^{-1}(\mathbf{x})\}^{-1}$ and $m_{pos} = C_{pos} \{C_\theta^{-1} m_\theta(\mathbf{x}) + \sum_{i:z_i=j} C_y^{-1}(\mathbf{x}) y_i\}$.

The cluster assignments z_i can be sampled from a discrete full conditional $p(z_i = j \mid \cdot)$

of the form:

$$\begin{cases} p(z_i = j \mid \mathbf{z}_{-i}, \alpha, \beta) p(y_i(\mathbf{x}) \mid \theta_j(\mathbf{x}), C_y), & j = 1, \dots, k^- \\ p(z_i = j \mid \mathbf{z}_{-i}, \alpha, \beta) \int p(y_i(\mathbf{x}) \mid \theta(\mathbf{x}), C_y) \mathcal{GP}(\theta(\mathbf{x}) \mid m_\theta(\mathbf{x}), C_\theta) d\theta, & j = k^- + 1 \end{cases}$$

$$\propto \begin{cases} p(z_i = j \mid \mathbf{z}_{-i}, \alpha, \beta) p(y_i(\mathbf{x}) \mid \theta_j(\mathbf{x}), C_y), & j = 1, \dots, k^- \\ p(z_i = j \mid \mathbf{z}_{-i}, \alpha, \beta) p(y_i(\mathbf{x}) \mid m_\theta(\mathbf{x}), C_y + C_\theta), & j = k^- + 1 \end{cases}.$$

If prior distributions for η_y^2 and $\eta_{\theta\ell}^2$ are set to $IG(\frac{a_\eta}{2}, \frac{b_\eta}{2})$, which denotes an inverse-gamma distribution with shape parameter a_σ and scale parameter b_σ , then the full conditional distribution for η_y is

$$IG\left(\frac{a_\eta + N|\mathcal{X}|}{2}, \frac{b_\eta + \sum_{i=1}^n \{y_i(\mathbf{x}) - \mu_i(\mathbf{x})\}^\top R_y^{-1}(\phi_y) \{y_i(\mathbf{x}) - \mu_i(\mathbf{x})\}}{2}\right)$$

where $R_y = \eta_y^{-2} C_y$, and the full conditional distribution for η_θ is

$$IG\left(\frac{a_\eta + K_n|\mathcal{X}|}{2}, \frac{b_\eta + \sum_{j=1}^{K_n} \{\theta_j(\mathbf{x}) - m(\mathbf{x})\}^\top R_\theta^{-1}(\phi_\theta) \{\theta_j(\mathbf{x}) - m(\mathbf{x})\}}{2}\right),$$

where $R_\theta = \eta_\theta^{-2} C_\theta$.

Finally, the prior mean m_θ has a conjugate Gaussian full conditional $N(m_{pos}, C_{pos})$:

$$C_{pos} = (K_n C_\theta^{-1} + C_m^{-1})^{-1}, \quad m_{pos} = C_{pos} \left\{ C_\theta^{-1} \sum_{j=1}^{K_n} \theta_j + C_m^{-1} m_m \right\}.$$

For parameters lacking conjugate priors, the Metropolis–Hasting algorithm (Dunson and Johndrow, 2020; Gelman et al., 2013) is employed. The posterior distributions are sampled using proposal distributions and acceptance probabilities by assigning suitable priors that reflect the analyst’s beliefs. Specifically, τ is assigned a Beta(a_τ, b_τ) prior, and its posterior is sampled using a Gaussian proposal distribution $\tau^* \mid \tau \sim N(\tau, 10^{-2})$. α is given a Gamma(a_α, b_α) prior, and a Gaussian proposal distribution $\alpha^* \mid \alpha \sim N(\alpha, 10^{-1})$ is employed for posterior sampling. Similarly, β is assigned a Beta(a_β, b_β) prior, and its posterior is sampled using a Gaussian proposal distribution $\beta^* \mid \beta \sim N(\beta, 10^{-1})$. The length-scale parameters ϕ_y and ϕ_θ of the covariance kernels are assigned inverse-gamma pri-

ors $\text{IG}(a_\phi, b_\phi)$; their posterior distributions are sampled using Gaussian proposal distributions $\phi_y^* | \phi_y \sim N(\phi_y, 10^{-1})$ and $\phi_\theta^* | \phi_\theta \sim N(\phi_\theta, 10^{-1})$, respectively.

4 Simulation

In this section, we evaluate the clustering performance and mean function estimation accuracy of the proposed method through numerical experiments and discuss its effectiveness.

4.1 Setting

First, we introduce the data-generating process along with the model in (6). The experiment contains data with different means depending on clusters. Specifically, observations across 40 areas for 15 days are assumed, with each day comprising 24 data points. In essence, 15 curve-like observations are gathered in 40 districts. We divided 40 areas into 8 groups, each containing 5 areas. For each group, a common mean structure θ_j , consisting of 24 points, was generated using $\mathcal{GP}(0, 2, 5)$, where $\mathcal{GP}(0, \eta, \phi)$ denotes a zero-mean Gaussian process with RBF kernel $K(x, x') = \eta^2 \exp(-|x - x'|^2 / \phi^2)$ with $x, x' \in \mathbb{R}$. Additionally, we sample y_{it} by adding μ_{it} to a noise, which was also generated in each region using either $\mathcal{GP}(0, 2/3, 1)$ or $\mathcal{GP}(0, 1, 1)$. The former is a high signal-to-noise ratio (SNR) case, whereas the latter is a low SNR case. This function is then added to the group mean. We posit that all the areas within the same cluster are adjacent. Hence, while each area has unique observations, they share a prominent trend within the cluster. Here, the primary objective is to formulate an approach for accurately classifying the generated data based on their general shapes and adjacency structures.

We generate 50 different datasets using the above-mentioned procedure and analyze each dataset using three clustering methods for functional data: the SGDP (our proposal), GDP, and SGDP with $\alpha\beta = 1$ (SDP, similarity-based Dirichlet process). The prior distributions for the range parameters, ϕ_y and ϕ_θ , and the scale parameters, η_y and η_θ , are set to $\text{IG}(1/2, 1/2)$ distribution. Concerning m_θ , a Gaussian process prior with mean $m_m = 1/2$ and covariance $C_m = 10I$ is utilized. For the SGDP and the SDP, the strength of neighboring relationships, τ , has a prior distribution $\text{Beta}(1/2, 1/2)$, and $\lambda(\cdot)$ in (5) is set to the identity function. In SDP, $\alpha \sim \text{Gamma}(1, 1)$ and $\beta = 1/\alpha$. Because the performances of the GDP and SGDP are dependent on the prior distributions of α and β , we implemented the following two cases of

Table 1: Adjusted Rand index (ARI), purity function (PF), and the root mean squared error (RMSE) for SDP, SGDP, and GDP with the different prior distributions.

SNR	Metric	SGDP		GDP		SDP
		Prior 1	Prior 2	Prior 1	Prior 2	-
Low	ARI	0.852	0.848	0.834	0.845	0.845
	PF	0.858	0.861	0.856	0.841	0.846
	RMSE	0.103	0.098	0.106	0.113	0.114
High	ARI	0.647	0.675	0.636	0.649	0.637
	PF	0.665	0.698	0.644	0.660	0.650
	RMSE	0.103	0.100	0.115	0.117	0.107

prior distributions based on the guidelines given at the end of Section 2.4:

$$\text{Prior 1 : } \alpha \sim \text{Gamma}(2, 1), \quad \beta \sim \text{Beta}(5, 1),$$

$$\text{Prior 2 : } \alpha \sim \text{Gamma}(5, 1), \quad \beta \sim \text{Beta}(20, 1).$$

The mean and variance of $\alpha\beta$ in Prior 1 are 1.667 and 1.508, and those in Prior 2 are 4.762 and 4.597, respectively. As measures of performance, we employ two widely used metrics to assess the clustering performance: the adjusted Rand index (Hubert and Arabie, 1985), abbreviated as ARI and the purity function (Manning et al., 2009), denoted by PF. These measures gauge the concordance between actual and predicted cluster allocations. Note that high values of both ARI and PF indicate a high clustering accuracy. Additionally, the accuracy of the mean function estimation is quantified using the root mean squared error (RMSE). All Bayesian methods employ burn-in and sampling periods of 16000 and 4000, respectively. Note that the effective sample sizes of the parameters of interest are at least 500.

4.2 Result

The results presented in Table 1, which presents the average of the evaluation metrics across the 50 datasets, provide an overview of the clustering performance. The findings demonstrate that the SGDP consistently outperforms the other methods. Specifically, the SGDP achieves the highest ARI values, indicating its superior clustering accuracy and consistency. This result suggests that the SGDP can effectively identify and group similar data points, even in the presence of noise and variability. Similarly, the SGDP attains the highest scores

Table 2: Posterior summaries of (α, β) .

SNR	Percentile	SGDP		GDP	
		Prior 1	Prior 2	Prior 1	Prior 2
Low	97.5%	(5.52, 0.22)	(4.29, 0.63)	(4.65, 0.48)	(4.75, 0.64)
	50%	(5.46, 0.20)	(4.25, 0.55)	(4.55, 0.31)	(4.68, 0.60)
	2.5%	(5.36, 0.19)	(4.22, 0.50)	(4.50, 0.25)	(4.54, 0.53)
High	97.5%	(5.58, 0.24)	(5.14, 0.56)	(4.86, 0.66)	(4.95, 0.79)
	50%	(5.53, 0.21)	(5.09, 0.53)	(4.83, 0.59)	(4.90, 0.71)
	2.5%	(5.47, 0.19)	(5.04, 0.42)	(4.76, 0.47)	(4.86, 0.62)

in terms of PF, particularly in high SNR scenarios. While SDP tends to discern minor differences and finely categorize them, the SGDP mitigates this tendency, striking a balance between capturing meaningful distinctions and avoiding over-segmentation. These results suggest that the SGDP is proficient in clustering data across different groups and accurately capturing the characteristics of each cluster. Furthermore, the SGDP exhibits the lowest RMSE values, which highlight its effectiveness in precise mean function estimation. Thus, the proposed SGDP is a robust and reliable choice for a wide range of clustering applications.

Table 2 summarizes the posterior distributions for the parameters α and β . The choice of prior distribution influences the posterior distribution of $\alpha\beta$ and attempts to increase $\alpha\beta$ in the prior distribution results in large posterior values. The posterior distributions of α and β were significantly larger than 1, and this tendency is more pronounced when Prior 2 is employed. This result, in conjunction with the findings presented in Table 1, suggests that higher $\alpha\beta$ values are instrumental in preventing the formation of excessive clusters, particularly in high SNR scenarios. This is an important consideration, as over-clustering can lead to a loss of interpretability of the results.

5 Application: Clustering hourly population data in Tokyo

In this section, we examine a case study involving population data from Tokyo, Japan, to investigate the efficacy of the proposed methodology. Initially, the characteristics of the population data are described. Subsequently, we explain models that capture the distinct features of the data. Lastly, we discuss the clustering results, focusing on the SDGP parameters and spatial correlation.

5.1 Hourly population data

The dataset under examination is population data collected by NTT Docomo Inc., the predominant mobile company in Japan with about 82 million users across the country. The company leverages user data to estimate the number of mobile phone users among all mobile carriers in each region. Based on observations and mobile phone penetration rates, the population of each region is estimated with a high degree of accuracy (Oyabu et al., 2013). In this study, we considered the seven special wards of Tokyo’s metropolitan area, with each mesh defined as a 500m² unit, resulting in $n = 452$ such units (refer to Figure 1). Hourly population data was collected within each mesh over $T = 30$ days, commencing on January 21, 2019. Recognizing that the variation in population flows reflected the unique characteristics of each region, we standardized the scales among the regions as follows:

$$\frac{y_{it}(x)}{\sqrt{\sum_{i,t} y_{it}^2(x)/n/T}}.$$

5.2 Model

Suppose we observe the function $y_{it}(x)$ on $x \in \mathcal{X}$ in the area $i \in \{1, 2, \dots, n\}$ and at time $t \in \{1, 2, \dots, T\}$. Analyzing functions observed across various points in time and space necessitates a methodology adept at capturing regions’ or periods’ specific attributes by identifying patterns.

Although our initial focus was on clustering based only on districts, we recognize that temporal data structures often contain information that should not be ignored and should be incorporated to glean deeper insights. This issue is addressed in the current section. We consider extensions that allow period-to-period cluster changes as follows:

$$y_{it}(x) \mid \mu_{it}(x) \sim \mathcal{GP}(\mu_{it}(x), C_y), \quad \mu_{it}(x) = \sum_{\ell=1}^M w_{t\ell} \left\{ \sum_{j=1}^{K_\ell} \theta_{j\ell}(x) I(z_{i\ell} = j) \right\}, \quad (7)$$

$$\theta_{j\ell}(x) \sim \mathcal{GP}(m_\theta^{(\ell)}, C_\theta^{(\ell)}), \quad j = 1, \dots, K_\ell, \quad \ell = 1, \dots, M,$$

where M is the number of periods, z_{i1}, \dots, z_{iM} represent the cluster membership variables, $w_{t\ell}$ denotes the period indicator, and $(m_\theta^{(\ell)}, C_\theta^{(\ell)})$ indicates the Gaussian process parameters for each period ℓ in each group j . If $T = M = 1$, (7) coincides with (6). Because the clusters

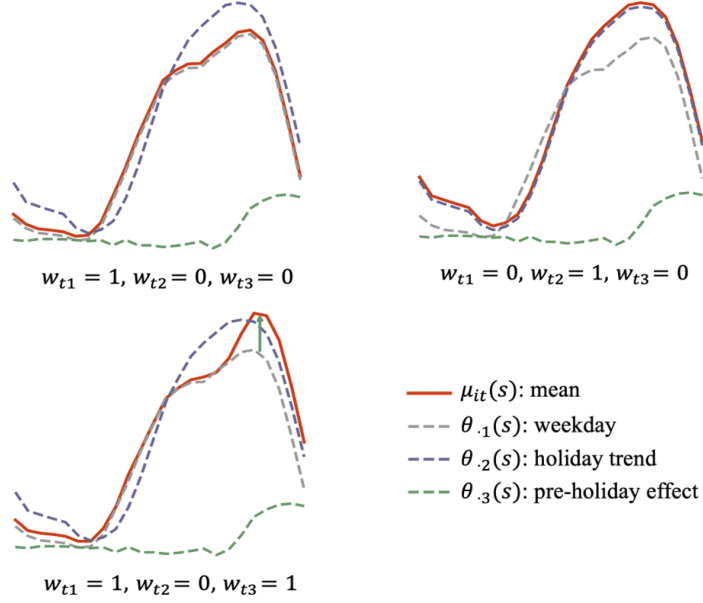


Figure 4: Weekday trend (top-left), holiday trend (top-right), and trend for the day before a holiday with the upward arrow indicating the pre-holiday effect (bottom-left).

depend on periods, the membership variables are given for each period; that is, we considered the prior distribution $(z_{1\ell}, \dots, z_{n\ell}) \sim \text{SGDP}(\alpha_\ell, \beta_\ell, \tau_\ell)$ for $\ell = 1, \dots, M$. Furthermore, we employed RBF kernels to model the covariance matrices C_y and $C_\theta^{(\ell)}$ for $\ell = 1, \dots, M$.

The notable distinction from (6) lies in the introduction of $w_{t\ell}$, which we elucidate here. Consider a scenario where $T = 2$, with day 1 being a weekday ($w_{t1} = 1, w_{t2} = 0$), and day 2 a holiday ($w_{t1} = 0, w_{t2} = 1$). The population flows on these days are markedly different between weekdays and holidays; hence, they are likely to exhibit varied clustering patterns. Additionally, Fridays may experience unique nighttime population increases in downtown areas compared to other weekdays, in which case $w_{t1} = 1, w_{t2} = 0, w_{t3} = 1$. The gray line in Figure 4 represents the weekday trend, the blue line represents the holiday trend, and the green line represents the pre-holiday effect. For instance, on Fridays, the observed data combines the weekday trend and the green line's effect (plus noise). This detailed temporal structure aids in deepening our understanding of spatial patterns. In our analysis, we set the number of periods M to three, with the weekday, holiday, and pre-holiday indicators for each period being w_{t1}, w_{t2} , and w_{t3} , respectively.

Table 3: Posterior summaries of $(\alpha_\ell, \beta_\ell)$ in the SGDP.

Percentile	Period		
	1	2	3
97.5%	(2.10, 0.96)	(1.06, 0.97)	(1.40, 0.96)
50%	(1.97, 0.94)	(1.05, 0.96)	(1.36, 0.95)
2.5%	(1.90, 0.93)	(1.05, 0.94)	(1.31, 0.93)

5.3 Implementation

We performed Bayesian inference based on the model reported in (7). The prior distributions for the range parameters of the covariance kernels, ϕ_y and $\phi_{\theta,\ell}$, along with the scale parameters, η_y and $\eta_{\theta,\ell}$, are all modeled using an $\text{IG}(1/2, 1/2)$ distribution for $\ell = 1, \dots, M$. For $m_\theta^{(\ell)}$, we employ a Gaussian process prior with mean $m_m^{(\ell)} = 1/2$ and covariance $C_m^{(\ell)} = 10I$ for each ℓ . τ follows $\text{Beta}(1/2, 1/2)$ prior distribution. The prior for α_ℓ is set as $\text{Gamma}(5, 1)$ and the prior for β_ℓ as $\text{Beta}(10, 1)$ to prevent generating excessive clusters for each ℓ , implying that the prior mean and variance of $\alpha_\ell\beta_\ell$ are equal to 4.545 and 4.338, respectively. Alongside the model in (7), we also implemented the SDP, whereby $\alpha_\ell \sim \text{Gamma}(1, 1)$ and $\beta_\ell = 1/\alpha_\ell$ for all ℓ , and GDP, where $\tau_\ell = 1$ in model (7). All the methods are implemented using the MCMC technique with a burn-in period of 16000 and a sampling period of 4000.

5.4 Effect of generalized parametrization

First, we analyze the differences between the SGDP and SDP by examining the distribution of the cluster numbers. Introducing priors leads to posterior estimates congruent with the data and prior beliefs, thereby reducing cluster numbers. Table 3 presents the posterior summaries of $(\alpha_\ell, \beta_\ell)$ in the SGDP. The posterior values of $\alpha_\ell\beta_\ell$ exceed 1 for each ℓ , and the results tend to avoid redundant clusters. The distributions of cluster size for these two methods in weekdays, holidays, and pre-holidays are illustrated in Figures 5, 6 and 7, respectively. From the weekday analysis in Figures 5, the SDP exhibits 8 out of 29 clusters consisting of only a single item, indicating a long tail to the right. Conversely, the SGDP shows a heavier left-side mass, resulting in a more attenuated tail. A similar pattern can be seen consistently across other periods. These findings suggest that owing to its flexible parametrization, the SGDP can effectively address the issue of over-clustering associated with increased dimensionality.

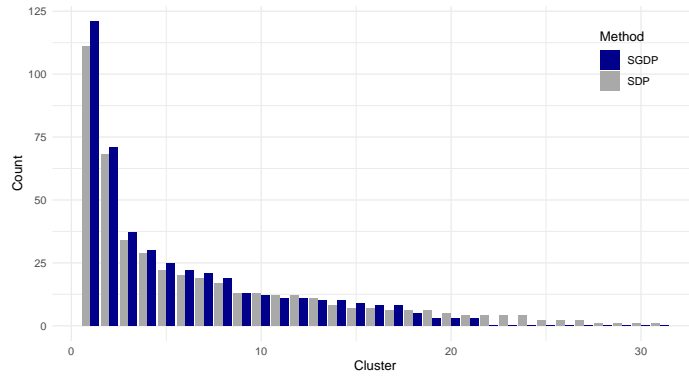


Figure 5: Distribution of the number of clusters for weekday obtained from the SGDP and SDP.

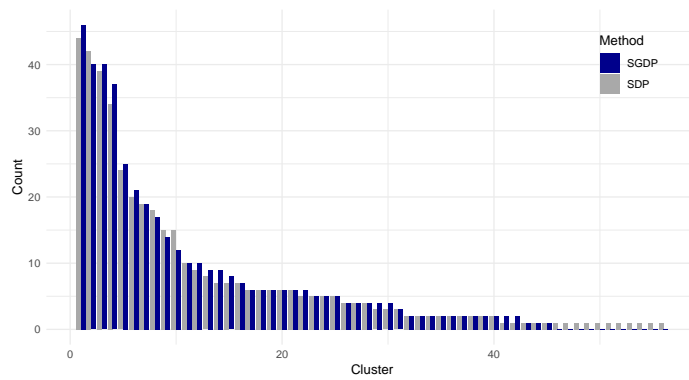


Figure 6: Distribution of the number of clusters for holidays obtained from the SGDP and SDP.

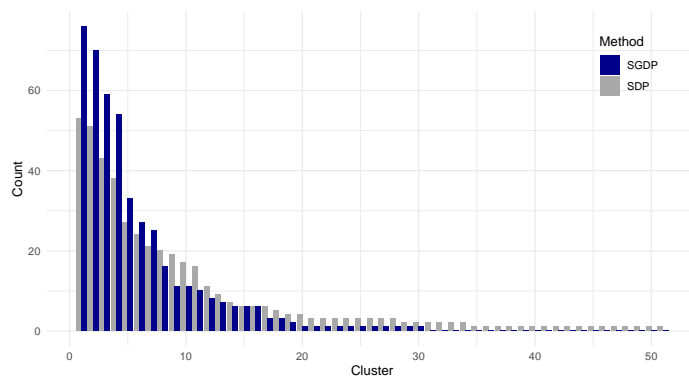


Figure 7: Distribution of the number of clusters for the pre-holiday effect obtained from the SGDP and SDP.

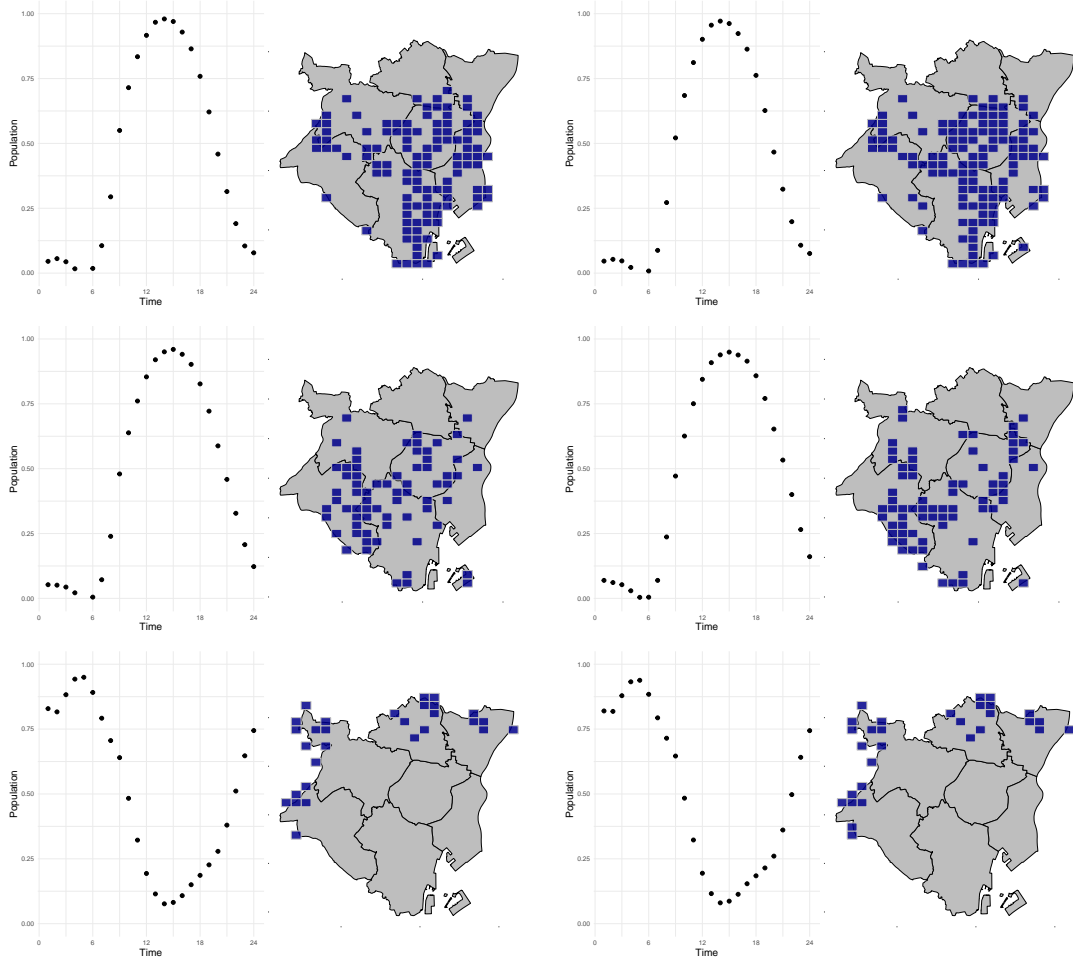


Figure 8: Three largest clusters on weekdays using the SDP (left) and the SGDP (right). Each row represents a different type of area: the top row is the office area, the middle row is the downtown, and the bottom row is the residential area.

Next, we examined the clusters on weekdays ($\ell = 1$) formed by the SGDP and SDP methods. Figure 8 depicts the three largest clusters on weekdays. The SDP-generated clusters are in the left column, while those generated by the SGDP are in the right column. The first row displays the weekday population flows in the business area and their corresponding mapped areas. The second and third rows represent downtown and residential areas, respectively. Evidently, the daytime population increases in the business and downtown areas, whereas it decreases in the residential areas, implying movement from residential to other areas for work or shopping, aligning with findings from other urban case studies (e.g., Xie et al., 2021). This result indicates that the two methods reflecting spatial information adequately capture regional characteristics.

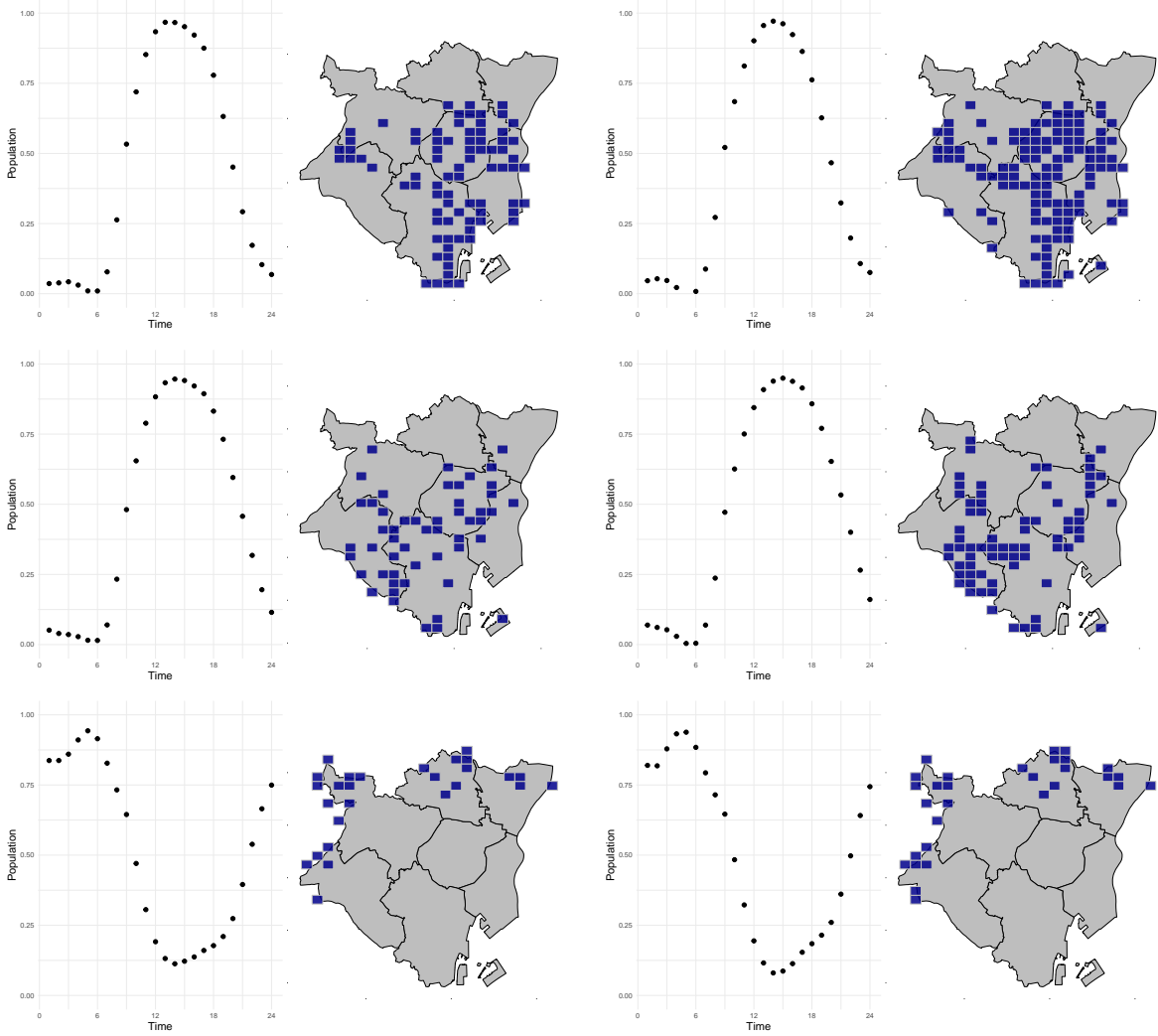


Figure 9: Three largest clusters on weekdays using simple GDP (left) and SGDP (right). Each row represents a different type of area: the top row indicates the office area, the middle row denotes the downtown area, and the bottom row highlights the residential area.

5.5 Spatial similarity

The previous clustering methods accounted for adjacencies. The resulting posterior means for (τ_1, τ_2, τ_3) were $(0.0097, 0.0176, 0.0125)$ for the SDP and $(0.0103, 0.0119, 0.0730)$ for the SGDP, indicating a notable correlation between geographically adjacent areas in the population data. To further examine this aspect, we compared the SGDP with the GDP. Figures 10–12 display the distributions of the SGDP and GDP. Both the methods produced approximately equal cluster numbers but differed in their proportions. As discussed in Section 2.3, this result indicates that the SGDP and GDP have identical probabilities of creating new clusters; however, the allocations within existing clusters differ. The detailed clusters

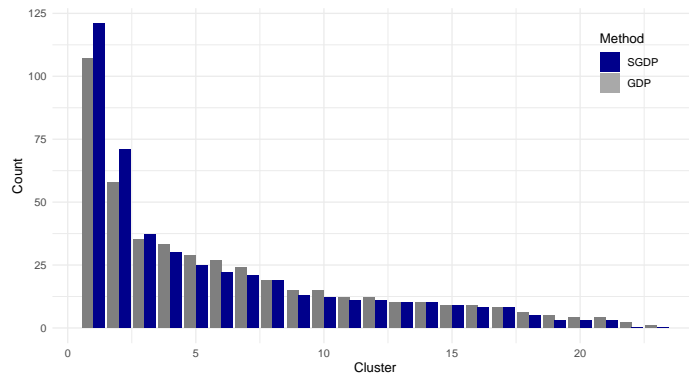


Figure 10: Distribution of the number of weekday clusters obtained from SGDP and GDP.

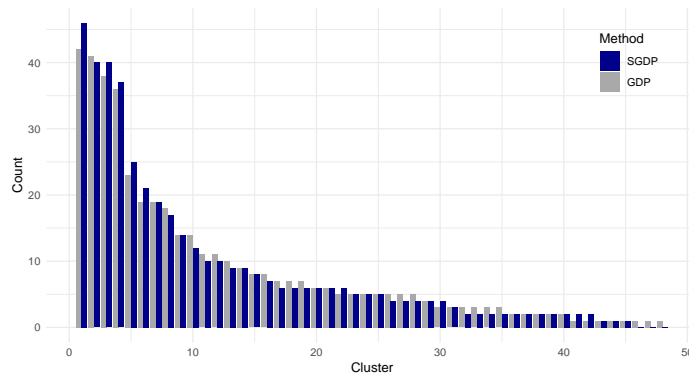


Figure 11: Distribution of the number of clusters for holiday obtained from SGDP and GDP.

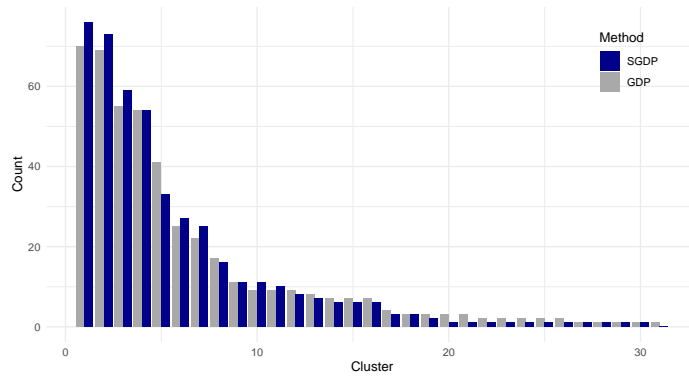


Figure 12: Distribution of the number of clusters for pre-holiday effect obtained from SGDP and GDP.

are shown in Figure 9, where the three rows correspond to the three types illustrated in Figure 8. The mean functions and clusters visible in the plots of the GDP are similar to those observed in the plots of the SGDP; however, they are relatively more dispersed than those of the SGDP. Notably, for the office and downtown areas, the clusters formed by the GDP overlook adjacent meshes owing to the absence of adjacency considerations. These findings underscore the importance of integrating spatial information into the methods.

6 Discussion

This paper introduces a nonparametric Bayesian clustering method that infuses pairwise similarity into the GDP framework, effectively addressing high-dimensionality and spatial correlations. The method mitigates excess clusters resulting from both DP characteristics and high dimensionality by setting a prior distribution of the GDP parameters. The correlation of adjacent data is reflected in the similarity, the strength of which can be determined through the posterior distribution.

Additionally, the method encompasses temporal structures, demonstrating the ability to accurately track population clusters. The organization of information in clustering can be extended to other contexts. In particular, the clusters and mean functions identified by our method can serve as factors in factor models for predicting population data, as exemplified in Wakayama and Sugasawa (2023). Future studies stand to benefit from methodologies that address temporal structure clustering for advanced practical applications.

Acknowledgments

This research was supported by JSPS KAKENHI (grant numbers 22J21090, 21H00699, 21K01421, 20H00080).

References

Ahmadi-Javid, A., O. Berman, and P. Hoseinpour (2018). Location and capacity planning of facilities with general service-time distributions using conic optimization. [arXiv preprint arXiv:1809.00080](https://arxiv.org/abs/1809.00080).

- Antoniak, C. E. (1974). Mixtures of Dirichlet Processes with Applications to Bayesian Nonparametric Problems. The Annals of Statistics 2(6), 1152 – 1174.
- Ayed, F., J. Lee, and F. Caron (2019, 09–15 Jun). Beyond the chinese restaurant and pitman-yor processes: Statistical models with double power-law behavior. In Proceedings of the 36th International Conference on Machine Learning, Volume 97, pp. 395–404. PMLR.
- Barcella, W., M. De Iorio, S. Favaro, and G. L. Rosner (2017, 09). Dependent generalized Dirichlet process priors for the analysis of acute lymphoblastic leukemia. Biostatistics 19(3), 342–358.
- Connor, R. J. and J. E. Mosimann (1969). Concepts of independence for proportions with a generalization of the Dirichlet distribution. Journal of the American Statistical Association 64(325), 194–206.
- Dahl, D. B., R. Day, and J. W. Tsai (2017). Random partition distribution indexed by pairwise information. Journal of the American Statistical Association 112(518), 721–732.
- Delaigle, A. and P. Hall (2012). Achieving near perfect classification for functional data. Journal of the Royal Statistical Society Series B: Statistical Methodology 74(2), 267–286.
- Dunson, D. B. and J. E. Johndrow (2020). The Hastings algorithm at fifty. Biometrika 107(1), 1–23.
- Ewens, W. J. (1972). The sampling theory of selectively neutral alleles. Theoretical population biology 3(1), 87–112.
- Ferguson, T. S. (1973). A Bayesian Analysis of Some Nonparametric Problems. The Annals of Statistics 1(2), 209 – 230.
- Ferguson, T. S. (1974). Prior distributions on spaces of probability measures. The Annals of Statistics 2(4), 615–629.
- Folland, G. B. (1999). Real analysis: modern techniques and their applications (2 ed.). New York: John Wiley & Sons.
- Gelfand, A. E. and A. F. Smith (1990). Sampling-Based Approaches to Calculating Marginal Densities. Journal of the American Statistical Association 85(410), 398–409.

- Gelman, A., J. B. Carlin, H. S. Stern, D. B. Dunson, A. Vehtari, and D. B. Rubin (2013). Bayesian Data Analysis (3 ed.). Chapman and Hall/CRC.
- Glynn, C., T. H. Byrne, and D. P. Culhane (2021). Inflection points in community-level homeless rates. The Annals of Applied Statistics 15(2), 1037–1053.
- Grazian, C. (2023). A review on Bayesian model-based clustering. arXiv preprint arXiv:2303.17182.
- Hjort, N. L. (2000). Bayesian analysis for a generalised Dirichlet process prior. Preprint series. Statistical Research Report.
- Hubert, L. and P. Arabie (1985). Comparing partitions. Journal of Classification 2, 193–218.
- Ishwaran, H. and L. F. James (2001). Gibbs Sampling Methods for Stick-Breaking Priors. Journal of the American Statistical Association 96(453), 161–173.
- Ishwaran, H. and M. Zarepour (2000, 06). Markov chain Monte Carlo in approximate Dirichlet and beta two-parameter process hierarchical models. Biometrika 87(2), 371–390.
- Korwar, R. M. and M. Hollander (1973). Contributions to the Theory of Dirichlet Processes. The Annals of Probability 1(4), 705 – 711.
- Lu, A. and A. Reddy (2012). Strategic Look at Friday Exceptions in Weekday Schedules for Urban Transit: Improving Service, Capturing Leisure Markets, and Achieving Cost Savings by Mining Data on Automated Fare Collection Ridership. Transportation research record 2274(1), 30–51.
- Lym, Y. (2021). Exploring dynamic process of regional shrinkage in Ohio: A Bayesian perspective on population shifts at small-area levels. Cities 115, 103228.
- MacEachern, S. N. and P. Müller (1998). Estimating mixture of dirichlet process models. Journal of Computational and Graphical Statistics 7(2), 223–238.
- Manning, C. D., H. Schütze, and P. Raghavan (2009). An introduction to information retrieval. Cambridge university press.

- Miller, J. W. and M. T. Harrison (2013). A simple example of Dirichlet process mixture inconsistency for the number of components. In Advances in Neural Information Processing Systems, Volume 26. Curran Associates, Inc.
- Miller, J. W. and M. T. Harrison (2014). Inconsistency of Pitman-Yor Process Mixtures for the Number of Components. Journal of Machine Learning Research 15(96), 3333–3370.
- Müller, P., F. A. Quintana, A. Jara, and T. Hanson (2015). Bayesian Nonparametric Data Analysis. Springer International Publishing.
- Nagata, T., S. Aoyagi, and H. Kawakami (2013). Using mobile spatial statistics for regional revitalization. NTT DOCOMO Technical Journal 14(3), 46–50.
- Neal, R. M. (2000). Markov Chain Sampling Methods for Dirichlet Process Mixture Models. Journal of Computational and Graphical Statistics 9(2), 249–265.
- Oyabu, Y., M. Terada, T. Yamaguchi, S. Iwasawa, J. Hagiwara, and D. Koizumi (2013). Evaluating reliability of mobile spatial statistics. NTT DOCOMO Technical Journal 14(3), 16–23.
- Páez, A. and D. M. Scott (2004). Spatial statistics for urban analysis: A review of techniques with examples. GeoJournal 61, 53–67.
- Pitman, J. (1995). Exchangeable and partially exchangeable random partitions. Probability Theory and Related Fields 102(2), 145–158.
- Pitman, J. (1996). Some developments of the Blackwell-MacQueen urn scheme. Lecture Notes-Monograph Series, 245–267.
- Pitman, J. and M. Yor (1997). The two-parameter Poisson-Dirichlet distribution derived from a stable subordinator. The Annals of Probability 25(2), 855 – 900.
- Pol, L. G. (1986). Marketing and the demographic perspective. Journal of Consumer Marketing 3(1), 57–65.
- Rasmussen, C. E. and C. K. I. Williams (2006). Gaussian Processes for Machine Learning. MIT press Cambridge, MA.

- Rodriguez, A. and D. B. Dunson (2014). Functional clustering in nested designs: Modeling variability in reproductive epidemiology studies. The Annals of Applied Statistics 8(3), 1416 – 1442.
- Sethuraman, J. (1994). A constructive definition of Dirichlet priors. Statistica Sinica 4(2), 639–650.
- Stutz, F. P. (2004). Charting urban travelers 24–7 for disaster evacuation and homeland security. In WorldMinds: Geographical Perspectives on 100 Problems: Commemorating the 100th Anniversary of the Association of American Geographers 1904–2004, pp. 177–182. Springer.
- Wakayama, T. and M. Imaizumi (2024). Fast Convergence on Perfect Classification for Functional Data. Statistica Sinica 34(4).
- Wakayama, T. and S. Sugawara (2023). Spatiotemporal factor models for functional data with application to population map forecast. arXiv preprint arXiv:2302.04412.
- Wang, M. and L. Mu (2018). Spatial disparities of Uber accessibility: An exploratory analysis in Atlanta, USA. Computers, Environment and Urban Systems 67, 169–175.
- Xie, C., D. Yu, X. Zheng, Z. Wang, and Z. Jiang (2021). Revealing spatiotemporal travel demand and community structure characteristics with taxi trip data: A case study of New York City. PLoS one 16(11), e0259694.
- Zhang, Y., Y. Fu, X. Kong, and F. Zhang (2019). Prefecture-level city shrinkage on the regional dimension in China: Spatiotemporal change and internal relations. Sustainable Cities and Society 47, 101490.